High pressure synthesis of the spin chain sulfide Ba 9 V 3 S 11 (S 2) 2

Batoul Almoussawi, Hayashi Tomohiri, Hiroshi Kageyama, Houria Kabbour

High pressure synthesis of the spin chain sulfide $Ba_9V_3S_{11}(S_2)_2$

Batoul Almoussawi[1], Hayashi Tomohiri[2], Prof. Hiroshi Kageyama[2], Dr. Houria Kabbour[1,*]

[1] *Univ. Lille, CNRS, Centrale Lille, ENSCL, Univ. Artois, UMR 8181 – UCCS – Unité de Catalyse et Chimie du Solide, F-59000 Lille, France.*

[2] *Department of Energy and Hydrocarbon Chemistry, Graduate School of Engineering, Kyoto University, Nishikyo-ku, Kyoto, 615-8510, Japan.*

* houria.kabbour@univ-lille.fr *http://uccs.univ-lille1.fr*

Abstract

The new compound $Ba_9V_3S_{11}(S_2)_2$ was synthesized using high pressure and high temperature. The single crystal XRD based structure solution and refinement show that it crystallizes in the hexagonal system with the space group $P\bar{6}c2$ (188) and the lattice parameters a= 9.1979(4) Å and c = 18.0462(10) Å. Its one-dimensional structure is related to the high-pressure phase $Ba_9V_3Se_{15}$ ($Ba_9V_3Se_{11}(Se_2)_2$) and consists of chains made of face-sharing VS_6 octahedra running along the *c*-axis. The chains contain two distinct sites of Vanadium with a mixed valence state of V^{3+} and V^{2+}. The space between the chains, two type of columns, is occupied by disulfides (S^{2-}) pairs and *isolated* sulfide anions S^{2-} surrounded by Ba^{2+} cations. The distributions within the columns are slightly different than in $Ba_9V_3Se_{11}(Se_2)_2$ making the two compounds not isostructural but polymorphs although they show the same symmetry and unit cell. We discuss this phase on the basis of crystallochemical analysis and DFT calculated electronic structure. Assuming a magnetic insulator as found from DFT+*U* calculations, we discuss the existence of magnetic clusters within the spin chains.

Introduction

Despite the numerous studies carried out for decades, chalcogenides continue to attract considerable attention due to their wide range of physico-chemical properties [1-2], such as magnetic, [3-4] electronic[5], NLO[6,7] , photocatalytic or photovoltaic properties for instance.

Especially, they may exhibit low-dimensional structuration and strongly correlated electronic systems leading to complex and exotic quantum ground states, superconductivity, charge and spin density waves, orbital ordering[8] *etc.*… In the system Ba-V-S, the $Ba_xV_6S_8$ (x = 0.41-0.48) phases consist of face-sharing distorted VS_6 octahedra forming a 3D framework and present a superconducting transition around 2.5 K [9]. In this chemical system, high pressure synthesis provides a way to favor other structural types which are metastable with non-conventional properties. It is the case of the *quasi*-one-dimensional hexagonal phase $BaVS_3$, based on face-sharing VS_6 octahedra forming spin-1/2 chains. It shows a weak anti-ferromagnetic behavior that switches to soft ferromagnetism with decreasing sulfur content[4]. $BaVS_3$ shows a complex behavior including several structural transitions, a metal-insulator transition and an incommensurate antiferromagnetic magnetic order. On another hand, the selenide analogue $BaVSe_3$ is quite different as it is a metallic ferromagnet below ~43 K. Their complex behavior can in addition be easily modified by chemical doping or by applying pressure. More recently, the selenide compound $Ba_9V_3Se_{15}$ with lattice parameters a = 9.5745(7) Å and c = 18.7814(4) Å in space group *P*-6*c*2 (188) was reported[10]. It was synthesized at high pressure and high temperature conditions (5.5 GPa and 1400°C) and exhibits similar face-shared VSe_6 chains. However, the separation between adjacent spin chains is larger than in $BaVSe_3$ with an interchain V-V distance of minimum 9.5745(7) Å due to a more complex interchain occupation. It is a semiconductor that shows a ferrimagnetic and a spin cluster glass transitions at 2.5 K and 3.3 K, respectively, under low magnetic field (10 Oe). The later disappear when the magnetic field exceeds 50 Oe. In the later system, a mixed valence of vanadium V^{3+}/V^{2+} is observed contrarily to $BaVS_3$ or $BaVSe_3$ containing V^{4+}, with strong influence on physical properties. Similarly, the iron based analogue sulfide $Ba_9Fe_3S_{11}(S_2)_2$[11] is reported and involves $2Fe^{3+}$ and $1Fe^{2+}$.

In the current study, we show the existence of the sulfide vanadium-based phase $Ba_9V_3S_{11}(S_2)_2$. The synthetic route appears more challenging than the selenide analogue as pointed by previous authors but we could isolate single crystals of this phase. Initially the single crystals were found in a preparation within the Ba-V-S-O system. Then, attempts to obtain a powder from the correct stoichiometry appeared challenging. Here, we describe its synthesis, structure solution and refinement based on single crystal XRD, crystalline structure, DFT electronic structure and make a comparison with other vanadium-based spin chains compounds.

Experimental section

Synthesis: Single crystals of $Ba_9V_3S_{15}$ were initially found in a preparation based on the precursors BaO/BaS/V/S. A mixture of the later precursors was grounded in an agate mortar in an Argon dry-glove box. The synthesis was carried out in a cubic-anvil high-pressure apparatus. The powder of the mixture was encapsulated into closed containers made up of boron nitride (BN) sleeve, and then embedded into solid pyrophyllite which transmit pressures typically up to several GPa to the sample. Pressure was slowly raised to 5 GPa, and the temperature to 800°C, then the conditions were kept for 60 minutes. The final product was a mixture of various phases including single crystals of $Ba_9V_3S_{15}$. Our attempts to synthesize a pure product from a stoichiometric mixture of the precursors BaS, V and S in similar high-pressure and high temperature (up to 1400°C) conditions did not allow to form the phase.

X-ray diffraction on single crystals diffraction was performed on a Rigaku XtaLab P200 diffractometer equipped with a Dectris Pilatus 200K detector and a Mo K_α source.

Scanning electron microscopy (SEM) experiments and EDX analysis were carried out on a S-3400N (Oxford instruments)

DFT calculations were carried out by employing the projector-augmented-wave [12,13] method encoded in the Vienna ab initio simulation package (VASP)[14] and the generalized gradient approximation (GGA) of Perdew, Burke and Ernzerhof[15] for the exchange correlation functionals. We employed GGA plus on-site repulsion U (GGA+U) method[16] to account for strong electronic correlation associated with the 3*d* states of V using the effective on-site repulsion of $U_{eff} = U - J = 3$ to 8 eV. A plane-wave cutoff energy of 600 eV and a threshold of the self-consistent-field energy convergence of 10^{-6} eV were used, with 232 k points in the irreducible Brillouin zone.

Results and discussion

Structure resolution

A black single crystal with a needle shape was selected for XRD data collection. The procedure is reported in table 1 with the data collection and refinement details. The unit cell

parameters *a* = 9.1979(4) Å and *c* = 18.0462(10) Å and the space group P $\bar{6}$c2 (188) were found. The refinement was carried out using JANA2006 program based on a structure solution obtained with the charge flipping method[17]. The EDX analysis carried out on the black needle shaped single crystals (SEM image and EDX spectrum of a typical single crystal are given in Fig. S1) led to the average atomic ratio 35.2/10.0/54.8 for Ba/V/S, respectively, in very good agreement with the refined composition $Ba_9V_3S_{15}$, (33/11/56).

The structure of $Ba_9V_3S_{11}(S_2)_2$ is shown in Fig.1 and 2. Atomic positions, anisotropic thermal parameters and interatomic distances are given in Table 2, 3 and 4. The structure consists of chains of face sharing octahedra VS_6 running along the *c*-axis giving the one-dimensional character of the structure (Figure 1.a). The chains contain two distinct vanadium sites that show slightly different set of V-S distances (see Table 4) which can be related to different valence states as will be discussed further from the DFT calculated magnetic moments. We assume a similar charge ordering tendency than the selenide analogue because we observe the same situation with a slightly higher average distance between V1 and its ligands. We however note that the difference between V1 and V2 environments is less pronounced in our case. $V1^{2+}$ is coordinated to six sulfur atoms S1 with dV1-S1 = 2.5236(34) Å and $V2^{3+}$ is coordinated to three atoms S2 and three atoms S1 with dV2-S2=2.5056(27) Å and dV2-S1=2.5292(63) Å. These V-S distances are longer than those found in $BaVS_3$, *i.e.* dV-S=2.3847(64)[18] but comparable to those found in the deficient phase $Ba_{0.5}V_8S_5$[19] (2.532 Å). V^{4+} in $BaVS_3$ lead to shorter distances than in the reduced form $Ba_{0.5}V_8S_5$ and the V^{3+}/V^{2+} based title phase. The arrangement of V1 and V2 within the chain is such that one octahedron $V1S_6$ alternates with two $V2S_6$, see Figure 1.c.This sequence results in variable V-V separations as sketched in Figure 1.d which also characterize the two different magnetic exchange paths.

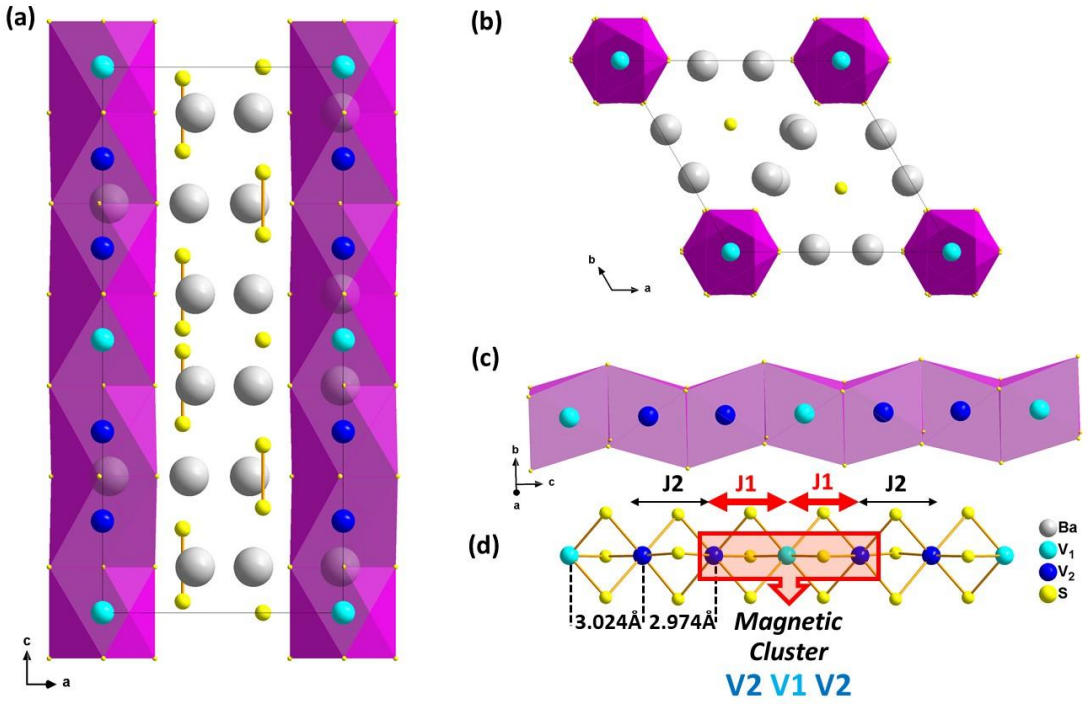

Figure 1. a) $Ba_9V_3S_{15}$ view along *b*-axis, b) $Ba_9V_3S_{15}$ view along *c*-axis c) VS_6 based one-dimensional chain d) arrangement of V1 and V2 in the spin chain showing strong J1 (magnetic coupling for V1-V2) and far weaker J2 (for V2-V2) magnetic exchange couplings. This interplay between J1 and J2 defines magnetic clusters with the sequence (V2-V1-V2).

The VS_6 based chains are arranged in a triangular lattice manner in the *ab* plane as shown in Figure 1.c and as found in $Ba_9V_3Se_{15}$. The space between the chains is occupied by barium cations surrounding sulfur-based columns running along the same direction than the chains. Two types of columns can be distinguished, see Figure 2.a. In the first column, S4 is half occupied (from this position S4-S4 distances of 0.7047(8) Å are generated). An ordered vision of those S4 sites to avoid short distances lead to either the formation of a disulfide pair with the adjacent S3 site, $d_{S3\text{-}S4}$ = 2.4038(65) Å, S3 distant of 3.4685(51) Å from next sulfur atom, an ordered scenario is given in Figure 2.d. In the second one, isolated S^{2-} anions S6 alternate with $(S_2)^{2-}$ disulfide pairs S5-S5 with a distance of 2.0663(33) Å. S6 is located in a $Ba1_6$ octahedron Figure 2.b The distances found within the disulfide pairs are comparable with those found in the iron based isotype $Ba_9Fe_3S_{15}$[20] with 2.037 and 2.547 Å for the shortest and the longest respectively.

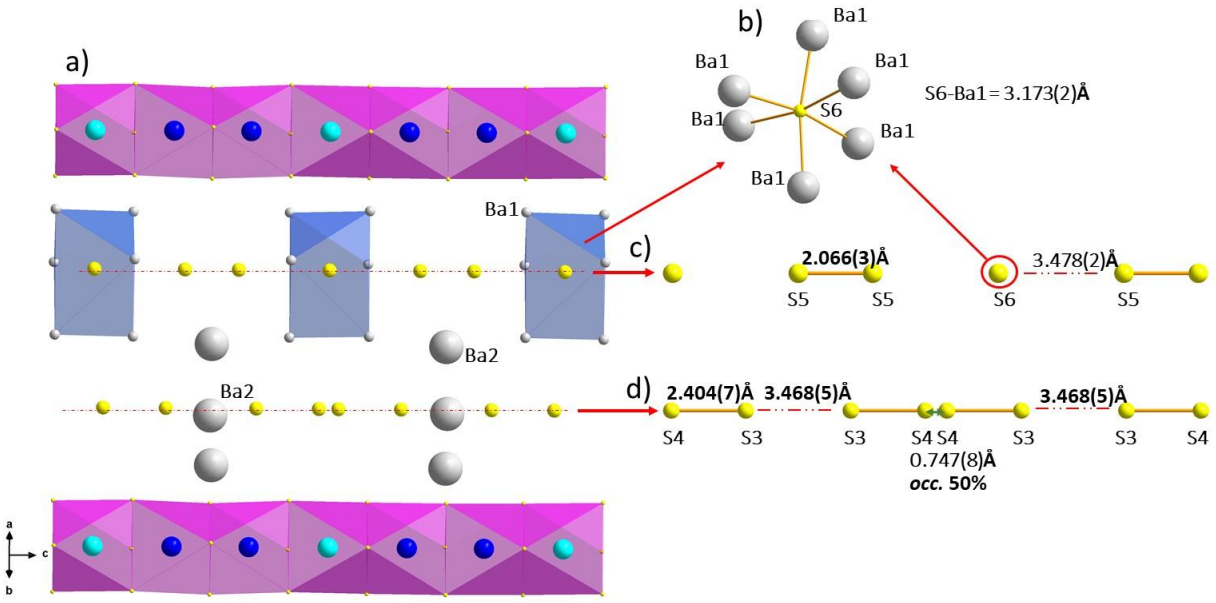

Figure 2 a) View of $Ba_9V_3S_{15}$, b) octahedron SBa_6 geometry, c-d) distribution of disulfide pairs and isolated sulfur anions within the columns

Sulfur distribution within the columns

The columns arrangement described above is slightly different from the one found in the selenide phase $Ba_9V_3Se_{15}$ as depicted in Figure 3. In the selenide phase, column 1 is ordered with diselenide pairs made of selenium atoms from a common 4*h* position and an isolated selenide in a 2*c* position. The disorder is found in column 2 with a split Se site inducing a Se-Se distance of ~1.90 Å imposing half occupancy, this site alternates with a fully occupied distinct 4*i* site, an ordered scenario imposes alternating diselenide pairs and isolated Se anions. Therefore, the two compounds are not isostructural due to different Wyckoff positions involved in the chalcogenide columns although they show the same symmetry, unit cell and framework (chains and Ba atoms). They can be considered as polymorphs. On another hand, $Ba_9Fe_3S_{15}$ is isostructural with the selenide phase with a similar sites distribution between column 1 and 2. We note however that the shortest/longest dichalcogenides pairs distances are found in column (1)/(2) in the Fe-compound while they are found in column (2)/(1) in the selenide phase.

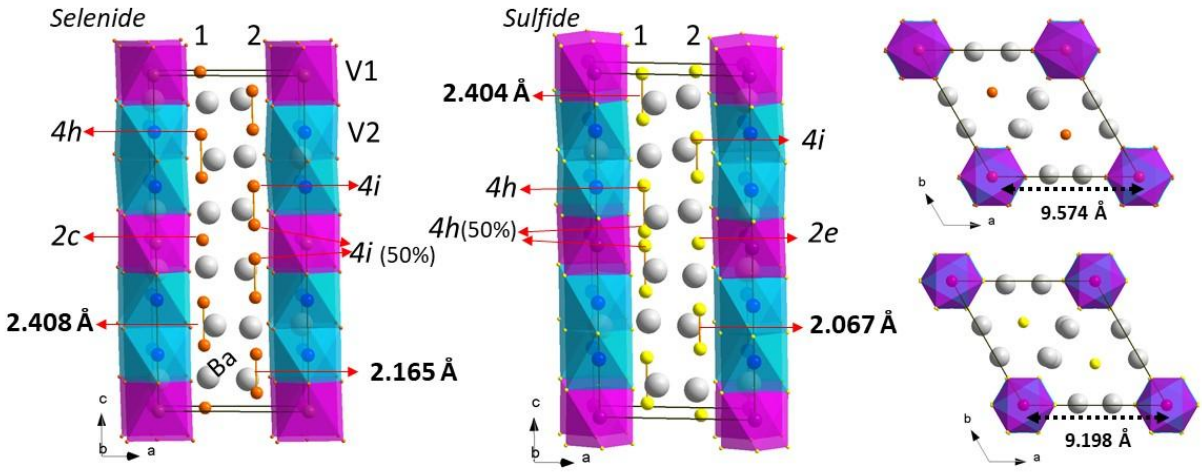

Figure 3. Comparison between the title phase and the selenide $Ba_9V_3Se_{15}$ highlighting the subtle difference of the arrangement within the (di)chalcogenides columns. On the right, projections in the *ab* plan showing the distances between two adjacent chains in both phases

DFT calculations

The electronic structure of the title phase was investigated using GGA+U calculations, the band structure and projected density of states are represented in Figure 4. The magnetic configurations considered in DFT+*U* here yield insulating states, we thus assume a magnetic insulator for the rest of the discussion. We have investigated several magnetic configurations including those studied by Zhang *et al.* for the selenide with similar U_{eff}= 5 value. Table 5 gathers the magnetic moments obtained for V1 and V2 for the different magnetic configurations. The FM gives 2.27 and 2.49 µB for V1 and V2, respectively, while the introduction of AFM interactions inverses the tendency and increases the difference between µ(V1) and µ(V2). For instance, the FIM configuration exhibits 2.74 and -2.20 µB for V1 and V2, respectively. For the selenide, 2.59 and -2.00 µB are reported for the FIM leading to a description of spin states for V1 and V2 being approximately S_1= 3/2 and S_2= 1. We can propose a similar scenario for all AFM-containing configurations but it doesn't hold for the FM. Regarding the band structure, its description is based on a lowered symmetry in *P*3*c*1 induced by the ordered structure that we built for the calculation (considering the split half occupied sulfur site). The structure was not relaxed to avoid slight geometrical changes in the spin chain especially in the lowered symmetry, that may affect the magnetic exchanges. Focusing on the top of the valence band (VB) and bottom of the conduction band (CB), the bands are flat except in the $\Gamma \rightarrow$ A direction, *i.e.* the k_z direction (of the chains) where they

are more dispersed thus reflecting the quasi-1D structure. On another hand, the PDOS allow visualizing the contribution of the different anionic species if we consider separately the S^{2-} of the VS_6 octahedra, the disulfide pairs (S_2) and the isolated sulfur within the interchain space. The $S_{(VS6)}$ states are hybridized with the vanadium states in the range of about -4.6 eV up to the Fermi level. The other anionic species have weak interactions with the framework. The two types of disulfide pairs with 2.0602(1) Å and 2.4404(1) Å S-S distances, show roughly similar DOS topologies but with different split in the major peaks and a higher dispersion for the shorter distance pair as expected from the stronger interaction within it.

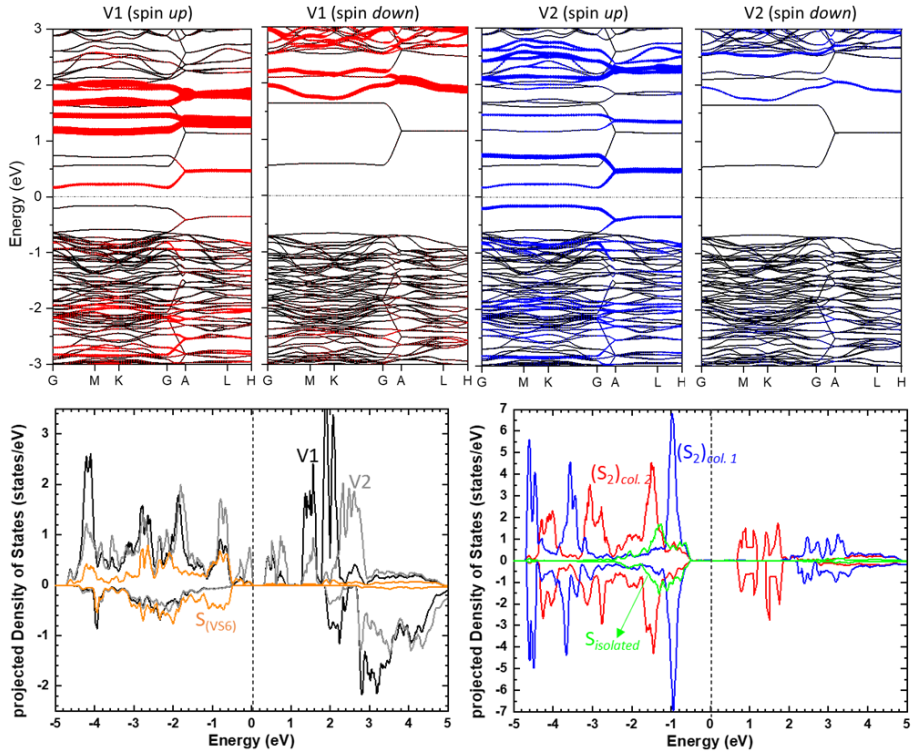

Figure 4. Total band structure and fat bands (in red for V1 and blue for V2) (top). Projected density of states (PDOS) of $Ba_9V_3S_{15}$ (bottom)

Using the procedure detailed in the supplementary information and the magnetic configurations represented in figure 5, we extracted from our DFT+U calculations the magnetic interactions constants *J*1 = 77.66 meV and *J*2 = 2.15 meV, considering U_{eff}= 5 eV as used for the selenide (see Table 6 for geometrical details of J1 and J2). We consider decoupled 1D spin chains with negligible interactions and estimate the intra-chain couplings. For the title phase, the calculated J and the relative energies of the magnetic configurations are dependent on the U choice, with J1 AFM below U= 3 eV and FM above. The ferromagnetic configuration becomes the most stable for U > 3eV and up to U= 8eV the

same tendency is observed. For the later range, J1 is much stronger in magnitude than J2, which allow to use a similar *cluster* description *V*(2)-*V*(1)-*V*(2) than for the selenide study[21] . Strong J1 interactions between V1 and V2 define the magnetic cluster while weak J2 (V2-V2 interactions) link those clusters (see Fig. 1d). Here, in absence of magnetic measurements it is difficult to draw conclusions on the expected behavior. Indeed, the reported magnetic systems in Ba-V-*X* (*X*= S, Se) show complex behaviors with multiple phenomena occurring upon temperature and pressure and their behaviors can be easily modified or suppressed upon slight chemical variations (doping, vacancies) as illustrated in the introduction. One more example is $Ba_{1-x}Sr_xVS_3$ that show an abrupt onset of ferromagnetic (FM) order at x=0.07[22].The magnetic cluster description should be a reasonable vision while further statements would need confrontation with experimental data.

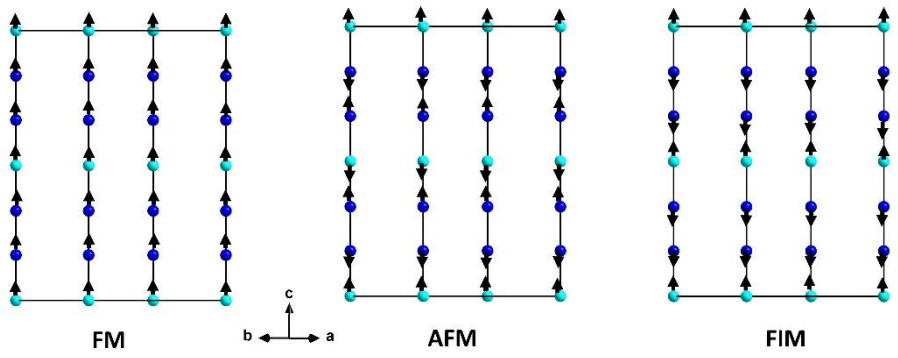

Figure 5. Different magnetic configurations of $Ba_9V_3S_{15}$ used in the DFT+*U* calculations. V1 is in light blue and V2 in dark blue, arrows represent spin up (↑) and spin down (↓).

Conclusion

The new phase $Ba_9V_3S_{15}$ could be stabilized using high pressure and high temperature in the form of single crystals. It belongs to the one-dimensional magnetic system $Ba_9M_3X_{15}$ (*M*= V, Fe and *X*= S, Se) that exhibits chains made of face-sharing MX_6 octahedra as found in $BaVX_3$ (X= chalcogenide). Two major structural features differentiate those two structural types: two distinct *M* sites are present in the former's chains while one site defines the chains in the later. Then, a higher separation between the magnetic chains with more complex interspace is found for $Ba_9M_3X_{15}$. It is made of columns of dichalcogenide pairs and chalcogenide anions alternating and surrounded by Barium cations. We show that the columns occupation by sulfur species is slightly different in the sulfide compared to the

selenide, making them polymorphs and not isostructural. Within the $Ba_9M_3X_{15}$ (*M*= V, Fe and *X*= S, Se), $Ba_9V_3S_{15}$ was targeted in previous work, we show here its experimental realization in the form of single crystals within a complex mixture. Using first-principles calculations, we show the formation of magnetic clusters within the spin chains. Then, extensive synthetic efforts are required to reach a polycrystalline sample of this metastable phase to experimentally investigate this hypothesis.

CCDC Deposition Number 2051748 contains the **supplementary crystallographic data** for the compound $Ba_9V_3S_{11}(S_2)_2$. These data are provided free of charge by the joint Cambridge Crystallographic Data Centre and Fachinformationszentrum Karlsruhe Access Structures service www.ccdc.cam.ac.uk/structures.

Acknowledgments

This work was supported by JSPS Core-to-Core Program (JPJSCCA20200004) and JSPS Kakenhi "Mixed-anion" (JP16H06438, JP16H6439, 16K21724). It was also supported by the French government through the Programme Investissement d'Avenir (I-SITE ULNE / ANR-16-IDEX-0004 ULNE) managed by the Agence Nationale de la Recherche (Project ANION-COMBO). The regional computational cluster supported by Lille University, CPER Nord-Pas-de-Calais/CRDER, France Grille CNRS and FEDER is thanked for providing computational resources. B. Almoussawi thanks University of Lille for financial support.

KEYWORDS: high pressure chemistry, mixed-valent compounds, DFT, polychalcogenides, spin chains

Table 1. Data collection and refinement details

Formula	$Ba_9V_3S_{15}$
Molecular weight (g. mol^{-1})	1869.8
Symmetry	*Hexagonal*
Space group	P -6 c 2 (188)
Unit cell dimensions (Å)	a = 9.1979(4) c=18.0462(10)
Volume ($Å^3$)	1322.19(11)
Z	2
Data Collection	

Equipment	Rigaku XtaLab P200
Λ [Mo K_α; Å]	0.71073
Calculated density (g cm^{-3})	4.6965
Crystal shape	Needle
Crystal dimensions (μm)	79×10×5
Color	Black
Absorption correction	analytical
Scan mode	ω, φ
θ (min−max) (°)	2.26-30.74
μ (mm−1 ; for λ Kα = 0.56087Å)	15.343
F(000)	1626
Reciprocal space recording	−8 ≤ h ≤ 13 −13 ≤ k ≤ 10 −25 ≤ l ≤ 24
No. of measured reflections	7128
No. of independent reflections	1315
I > 3σ(I) (total)	1222
Refinement	
Number of refined parameters	46
Refinement method	Least-squares
Weighting scheme	sigma
R1(F) [I > 3σ(I)]/R1(F^2) (all data, %)	0.0298/0.0327
w$R2(F^2)$ [I > 3σ(I)]/w$R2(F^2)$ (all data, %)	0.0888/0.0909
Goodness of Fit	1.70
Max/Min residual electronic density ($e^-/Å^3$)	1.97/ -3.11

Table 2. Atomic positions and isotropic thermal displacement for $Ba_9V_3S_{15}$

Atom	Wyck.	S.O.F	X	Y	Z	U_{eq}
Ba1	12l		0.62727(8)	0.01242(13)	0.08393(2)	0.0136(2)
Ba2	6k		0.02774(8)	0.38827(9)	1/4	0.0108(3)
V1	2a		0.00000	0.00000	0.00000	0.0101(7)
V2	4g		0.00000	0.00000	0.16808(12)	0.0109(5)
S1	12l		0.2177(4)	-0.0039(8)	0.08378(9)	0.0122(9)
S2	6k		0.2262(4)	0.2131(5)	1/4	0.0117(11)

S3	4i		0.333333	0.666667	0.1539(2)	0.0281(11)
S4	4h	0.5	0.333333	0.666667	0.0207(3)	0.0204(16)
S5	4g		0.666667	0.333333	0.19275(13)	0.0015(5)
S6	2e		0.666667	0.3333333	0.00000	0.0043(8)

Table 3. ADP harmonic parameters Uij (Å²) for $Ba_9V_3S_{15}$

Atom	**U_{11}**	**U_{22}**	**U_{33}**	**U_{12}**	**U_{13}**	**U_{23}**
Ba1	0.0130(3)	0.0133(3)	0.0164(3)	0.0079(3)	0.00097(15)	0.00170(12)
Ba2	0.0069(4)	0.0105(3)	0.0158(3)	0.0050(3)	0.00000	0.00000
V1	0.0108(8)	0.0108(8)	0.0087(13)	0.0054(4)	0.00000	0.00000
V2	0.0096(5)	0.0096(5)	0.0134(9)	0.0048(3)	0.00000	0.00000
S1	0.0110(13)	0.0107(8)	0.0134(8)	0.0044(13)	0.0013(6)	0.0008(4)
S2	0.0097(16)	0.0117(15)	0.0152(11)	0.0064(10)	0.00000	0.00000
S3	0.0208(12)	0.0208(12)	0.043(2)	0.0104(6)	0.00000	0.00000
S4	0.0221(18)	0.0221(18)	0.017(3)	0.0111(9)	0.00000	0.00000
S6	0.0027(10)	0.0027(10)	0.0075(15)	0.0013(5)	0.00000	0.00000

Table 4. Main distances (Å) for $Ba_9V_3S_{15}$

Atoms 1,2	**d 1,2 (Å)**	**Atoms 1,2**	**d 1,2 (Å)**
Ba1—S2	3.2672(11))×2	Ba2—S4	3.059(7)

Ba1—S4	3.326(4)×2	Ba2—S6	3.2283(18)
Ba1—S5	2.979(5)	Ba2—S1	3.182(2)
Ba1—S5	3.028(5)	V1—S1	2.5236(62) ×6
Ba1—S6	3.204(2) ×2	V2—S1	2.5292(63) ×3
Ba2—S3	3.1731(11)	V2—S2	2.5056(27) ×3
Ba2—S4	3.006(6)	S3—S3	3.4685(5)
S4—S4	0.7471(77)	S3—S4	2.4038(65)
S5—S5	2.0663(33)	S5—S6	3.4784(24)

Table 5. DFT+*U* calculated magnetic moments for V1 and V2 on different magnetic configurations

U_{eff}= 5 eV	μ_{FM} (μB)	μ_{AFM} (μB)	μ_{FIM} (μB)
V1	2.27	2.79	2.74
V2	2.49	2.10	2.20

Table 6. Description of the geometry around J1 and J2 interactions

	Atom1	Atom2	$d_{[1,2]}$ (Å)	V-S…S-V	V-S-V (°)
J1	V1	V2	3.033(2)	V1-S1=2.524(3) S1-V2=2.529(6)	V1-S1-V2= 73.78°
J2	V2	V2	2.957(3)	V2-S2= 2.506(4) S2-V2= 2.506(4)	V2-S2-V2= 72.32°

REFERENCES

(1) Y.-Y. Li, H. Wang, B.-W. Sun, Q.-Q. Ruan, Y.-L. Geng, P.-F. Liu, L. Wang, L.-M. Wu, *Cryst. Growth Des.* **2019**, *19* (2), 1190–1197.

(2) L. Zhang, D. Mei, Y. Wu, C. Shen, W. Hu, L. Zhang, J. Li, Y. Wu, X. J. He, *Solid State Chem.* **2019**, *272*, 69–77.

(3) H. A. Katori, T. Adachi, H. Ohta, S. Nakamura, A. Fuwa, *Phys. Procedia* **2015**, *75*, 552–556.

(4) N. J. Poulsen, *Mater. Res. Bull.* **1998**, *33* (2), 313–322.

(5) K. Ishida, Y. Ikeuchi, C. Tassel, H. Takatsu, C. M. Brown, H. Kageyama, *Inorganics* **2019**, *7* (5), 63.

(6) Y.-Y. Li, P.-F. Liu, L.-M. Wu, *Chem. Mater.* **2017**, *29* (12), 5259–5266.

(7) F. Liang, L. Kang, Z. Lin, Y. Wu, *Cryst. Growth Des.* **2017**, *17* (4), 2254–2289.

(8) S. Fagot, P. Foury-Leylekian, S. Ravy, J. P. Pouget, M. Anne, G. Popov, M. V. Lobanov, M. Greenblatt, *Solid State Sci.* **2005**, *7* (6), 718–725.

(9) O. Fuentes, H. Wang, B. H. Ward, J. Zhang, D. M. Proserpio, F. Calvagna, C. E. Check, K. C. Lobring, C. Zheng, *Chem. Mater.* **2001**, *13* (9), 3051–3056.

(10) J. Zhang, M. Liu, X. Wang, K. Zhao, L. J. Duan, *Phys. Condens. Matter* **2018**, *4*, 1–10.

(11) A. B. Blake, *Acta Crystallogr. Sect. B Struct. Crystallogr. Cryst. Chem.* **1982**, *38* (1), 348–349.

(12) P. E. Blöchl, *Phys. Rev. B* **1994**, *50* (24), 17953–17979.

(13) G. Kresse, D. Joubert, *Phys. Rev. B* **1999**, *59* (3), 1758–1775.

(14) G. Kresse, D. Vogtenhuber, M. Marsman, M. Kaltak, F. Karsai, M. Schlipf, Vienna ab-initio simulation package (VASP) https://www.vasp.at.

(15) J. P. Perdew, K. Burke, M. Ernzerhof, *Phys. Rev. Lett.* **1996**, *77* (18), 3865–3868.

(16) S. L. Dudarev, G. A. Botton, S. Y. Savrasov, C. J. Humphreys, A. P. Sutton, *Phys. Rev. B* **1998**, *57* (3), 1505–1509.

(17) V. Petříček, M. Dušek, L. Palatinus, *Zeitschrift für Krist. - Cryst. Mater.* **2014**, *229* (5), 345–352.

(18) R. A. Gardner, M. Vlasse, A. Wold, *Acta Crystallogr. Sect. B Struct. Crystallogr. Cryst. Chem.* **1969**, *25* (4), 781–787.

(19) S. PETRICEK, H. BOLLER, K. KLEPP, *Solid State Ionics* **1995**, *81* (3–4), 183–188.

(20) H. Y. Hong, H. J. Steinfink, *Solid State Chem.* **1972**, *5* (1), 93–104.

(21) P. Foury-Leylekian, P. Leininger, V. Ilakovac, Y. Joly, S. Bernu, S. Fagot, J. Pouget, *Phys. B Condens. Matter* **2012**, *407* (11), 1692–1695.

(22) A. Gauzzi, N. Barišic, F. Licci, G. Calestani, F. Bolzoni, P. Fazekas, E. Gilioli, L. Forró, *cond-mat* **2006**, *1*, 2–5.

GRAPHICAL ABSTRACT

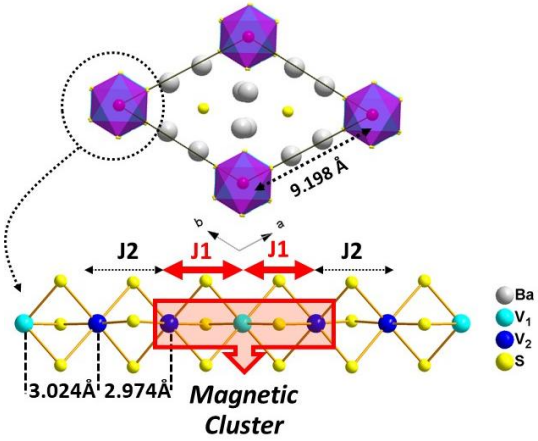

TABLE OF CONTENTS

The new high-pressure phase $Ba_9V_3S_{11}(S_2)_2$ exhibits a 1D-structure consisting of spin chains made of face-sharing VS_6 octahedra with two distinct Vanadium sites and a mixed valence V^{2+}/V^{3+}. The inter-chains space is occupied by disulfide pairs $(S_2)^{2-}$ and sulfide anions S^{2-} surrounded by Ba^{2+} cations. The relative strengths of J1 and J2 magnetic exchanges lead to a magnetic cluster description.